JOURNAL OF QUATERNARY SCIENCE (2026) **41**(5) 770–783 ISSN 0267-8179. DOI: 10.1002/jqs.70081

JQS Journal of Quaternary Science QRA Quaternary Research Association

Marine Isotope Stage 4 glaciation in northern England, UK: Evidence from Victoria Cave, North Yorkshire

TOM C. LORD,[1] PETER WILSON,[2]* JOYCE LUNDBERG,[3] ADRIAN P. PALMER,[4] MATT W. TELFER,[5] RHIANNON E. STEVENS,[6] PHILLIP J. MURPHY[7] and MARK LEWIS[8]

[1]Lower Winskill, Langcliffe, Settle, North Yorkshire, UK
[2]School of Geography and Environmental Sciences, Ulster University, Coleraine, Co. Londonderry, UK
[3]Department of Geography and Environmental Studies, Carleton University, Ottawa, ON, Canada
[4]Centre for Quaternary Research, Department of Geography, Royal Holloway, University of London, Egham, Surrey, UK
[5]School of Geography, Earth and Environmental Sciences, University of Plymouth, Plymouth, UK
[6]Institute of Archaeology, University College, London, UK
[7]School of Earth and Environment, University of Leeds, Leeds, UK
[8]Centre for Human Evolution Research (CHER), Natural History Museum, London, UK

Received 27 September 2025; Revised 29 April 2026; Accepted 2 May 2026

ABSTRACT: Victoria Cave, north Yorkshire, England, contains a long sequence of Pleistocene clastic sediments and calcite flowstones. Earlier work, using U–Th dating, established that the flowstone units formed in interglacial stages corresponding to Marine Isotope Stages (MIS) 13, 11, 9, 7 and 5. The intervening laminated sediments were therefore assigned to glacial stages (MIS 12, 10, 6 and 2) and regarded as rhythmites that settled from ponded glacial meltwater in the cave. Victoria Cave is a rare instance of cave rhythmites that formed over a number of glacial–interglacial cycles. The macro- and micromorphologies of the rhythmites support the above interpretation, and the mineralogy demonstrates that the sediments probably derive from rock types within the local area. An OSL age of 66 ± 8.4 ka from the uppermost unit of the rhythmites and two ^{14}C ages of 46.1–54.9 cal. ka BP and 48.9–>55.0 cal. ka BP, for horse and reindeer, respectively, from the overlying Bone-bearing Cave Earth provide a new chronology for these Late Pleistocene sediments. Together, these results indicate that the youngest rhythmites in Victoria Cave formed during MIS 4 and not MIS 2 as previously assumed. This provides strong support for more widespread glaciation in northern England in MIS 4 (~71–59 ka) than has previously been recognised. The MIS 4 rhythmites represent the most tightly constrained cave rhythmites in Britain and the first terrestrial-based evidence from this area for glaciation at that time. © 2026 The Author(s). *Journal of Quaternary Science* Published by John Wiley & Sons Ltd.

KEYWORDS: AMS ^{14}C dating; cave rhythmites; MIS 4 glaciation; OSL dating; Victoria Cave

Introduction

Victoria Cave (British national grid reference SD 838 650; 54.08° N, 02.25° W) is part of a relict phreatic cave system that opens to the surface at 440 m above sea level in a limestone fault scarp on the eastern side of the Ribble valley (Ribblesdale), ~2 km northeast of Settle, North Yorkshire (Fig. 1(A), (B)). It is a glacially truncated remnant of a more extensive system copiously filled by Pleistocene clastic sediments and calcite (Tiddeman, 1875; Lundberg et al., 2010; Fig. 2). Waltham (2013) suggests that Victoria Cave had formed within limestones exposed to the surface by ~1.3 Ma, and estimates for the oldest flowstones on the cave floor reveal that it had already drained by ~600 ka (Lundberg et al., 2010). The cave entrance lies in the side of a glacially modified dry valley, and beneath a ~30 m-high cliff composed of well-jointed and bedded limestone providing a plentiful source of clasts for scree accumulation on the slopes below (Fig. 3). The present dimensions of the cave (~50 × 30 × 15 m) are entirely the result of large-scale excavations from 1870 to 1878, during which time, much of the Quaternary succession was removed (Lundberg et al., 2010; Lord et al., 2012; Fig. 4). Archives from these investigations supplemented by casual interventions in the 1930s remain fundamental to research about the cave (Gascoyne et al., 1981; Hedges et al., 1992; Dearne and Lord, 1998; Gilmour et al., 2007; Lord et al., 2007; Lundberg et al., 2010; Jacobi and Lord, 2011; O'Connor and Lord, 2013). The clastic sediments include laminated units that have not previously been subject to detailed investigation, and little is known about their origin and age. The aims of this paper are therefore (i) to establish the nature of selected characteristics of the laminated sediments; (ii) to assess the most likely sources of and means by which the sediments accumulated; and (iii) to determine sediment age and the implications thereof.

*Correspondence: P. Wilson, as above.
Email: p.wilson@ulster.ac.uk

The Quaternary stratigraphy

The 1870s excavation archive, along with extant sections of undisturbed material, enabled Lundberg et al. (2010) to compile a detailed stratigraphic sequence of the cave sediments. This stratigraphy, outlined in Figs. 2 and 5, indicates four laminated clay units, two bone-bearing cave earths with Pleistocene mammal bones, roof-fall deposits and intervening calcite flowstones. Thermal ionisation mass spectrometer (TIMS) U–Th dating of the flowstones allowed

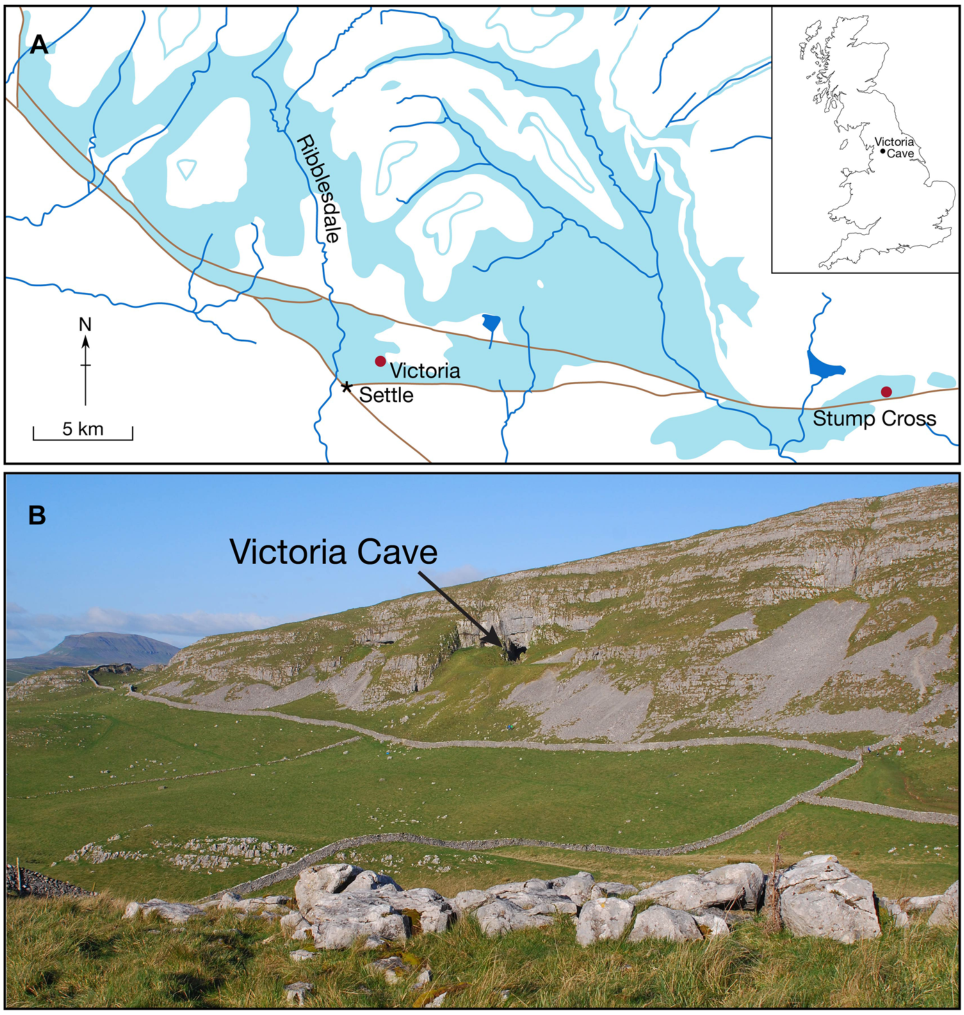

Figure 1. (A) Locations of Victoria Cave and Stump Cross Caverns, outcrop of Carboniferous limestone (pale blue) and the system of Craven Faults (brown lines) in North Yorkshire. (B) View of Victoria Cave in the face of Langcliffe Scar. The grassed-over slopes below the cave mouth are the spoil tips from the large-scale excavations of 1870–1878. [Color figure can be viewed at wileyonlinelibrary.com]

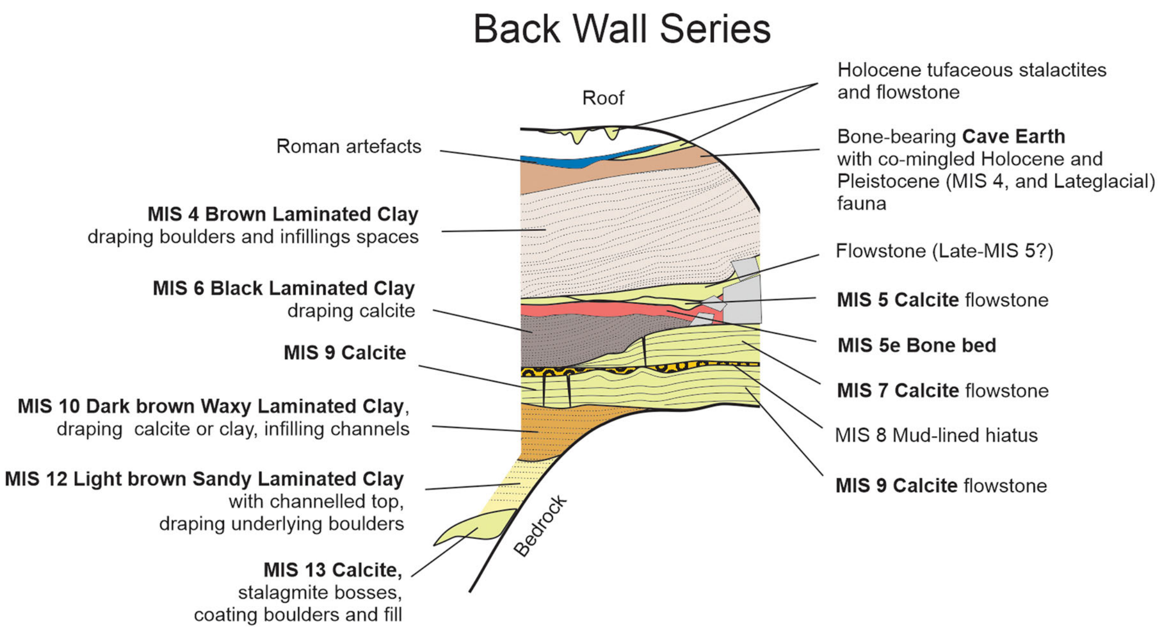

Figure 2. Copious and complicated sedimentary sequence of Victoria Cave over the last ~500 000 years, including clastic material, calcite and abundant faunal remains. This section (modified from Lundberg et al., 2010) is from the back wall of the main cave (see the location in Fig. 4—Back Wall Series). Note that the Bone-bearing Cave Earth and Brown Laminated Clay have been re-interpreted in light of the results of this present study, as outlined below in Results and Discussion. [Color figure can be viewed at wileyonlinelibrary.com]

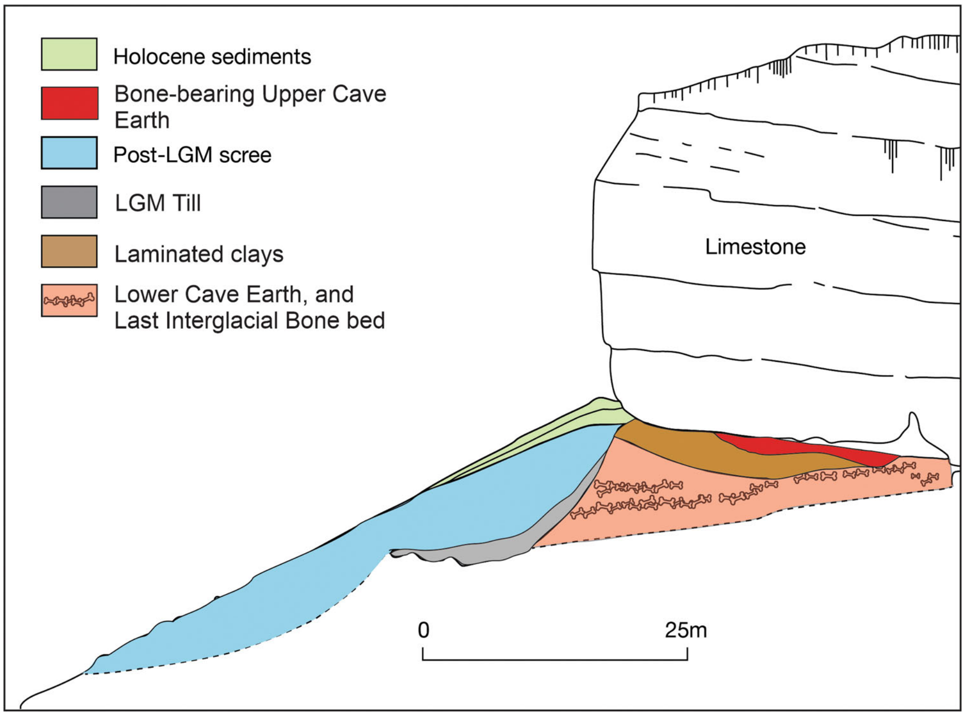

Figure 3. Sediments and stratigraphy at Victoria Cave (redrawn with modifications from Tiddeman (1875)). The sequence as depicted does not extend below the Lower Cave Earth/Last Interglacial Bone bed (MIS 5e) and the cave mouth is blocked by laminated clays assumed by Lundberg et al. (2010) to be of MIS 2 age on the basis of position above the MIS 5e Bone bed, but now attributed to MIS 4 in this paper. Sediments of the Entrance Series (Fig. 4) are now just outside the cliff line, but would have been inside before cliff recession in the Lateglacial and Holocene. [Color figure can be viewed at wileyonlinelibrary.com]

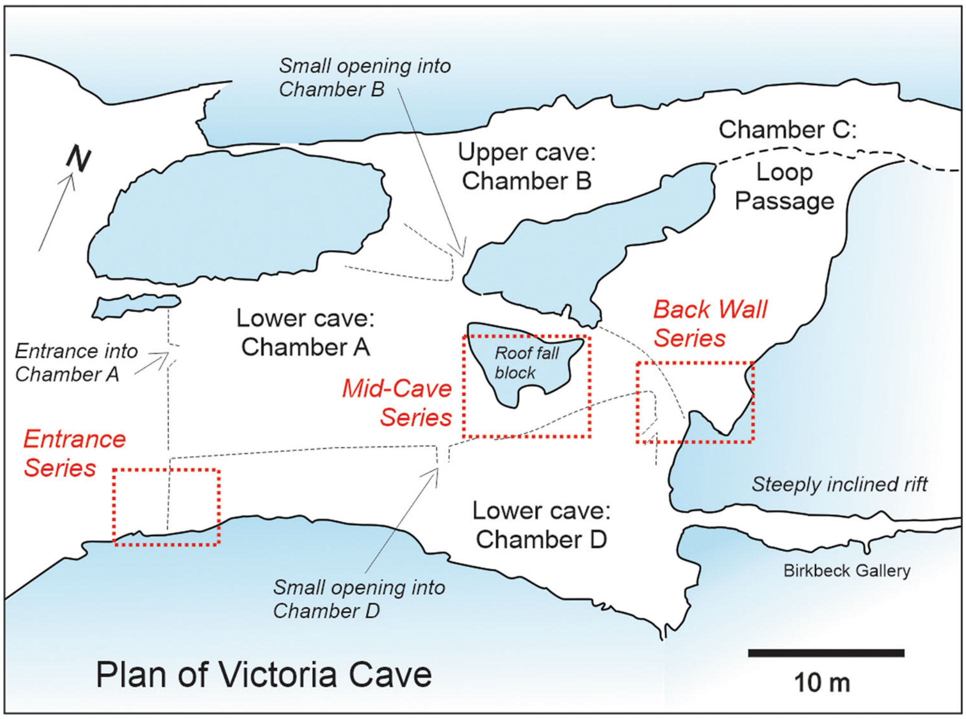

Figure 4. Plan of Victoria Cave based on a survey by the Lancaster University Archaeological Unit (Quartermaine, 1995). The angular dashed lines, in black, show the excavations by Tiddeman. The rectangular boxes show the locations of the three main sedimentary series that were reported by Tiddeman and studied over the years by Gascoyne et al., 1981; Hedges et al., 1992; Dearne and Lord, 1998; Gilmour et al., 2007; Lord et al., 2007; Lundberg et al., 2010; Jacobi and Lord, 2011; and O'Connor and Lord, 2013. The focus of this current study is the Mid-Cave Series. [Color figure can be viewed at wileyonlinelibrary.com]

the sequence to be tied to the Marine Isotope Stage (MIS) chronology. The dating demonstrated that flowstone formation occurred during interglacial stages, that is, MIS 13, MIS 11, MIS 9, MIS 7 and MIS 5. The four laminated clay units were therefore assigned to MIS cold stages, that is, MIS 12, MIS 10, MIS 6 and MIS 2 (note that there is no laminated unit equivalent to MIS 8) on the basis of their stratigraphic relationships to the dated flowstones (Lundberg et al., 2010). Assigning the uppermost unit of laminated clay to MIS 2, as opposed to MIS 4 or MIS 3, was based on evidence for an extensive cover of glacial ice at that time across northern England (cf. Chiverrell and Thomas, 2010; Hibbert et al., 2010).

The laminated sediments have not previously been subjected to the same degree of intensive research as the Pleistocene faunas and flowstones (Gascoyne et al., 1981; Gilmour et al., 2007; Lord et al., 2007; Lundberg et al., 2010; Jacobi and Higham 2011; Jacobi and Lord 2011; O'Connor and Lord 2013; Edwards et al., 2014). Tiddeman (1873, 1875, 1876, 1877, 1878) proposed that the sediments had accumulated in still water ponded by ice that blocked the cave entrance. In contrast, Murphy and Lord (2003) argued that the sediments had much in common with those recorded by Bull (1981) from caves in South Wales and for which translatory flow through bedrock fissures into a subterranean lake was the likely means of deposition. Because the laminated sediments resemble classic varve deposits, Lundberg et al. (2010) rejected the proposition of Murphy and Lord (2003), and considered them to be glaciolacustrine sediments that accumulated when the Ribblesdale valley glacier blocked the cave entrance and provided a source of sediment-rich meltwater from which the couplets settled, probably on an annual basis.

Methods

From Victoria Cave, three exposures of laminated sediment from the Mid-Cave Series of Lundberg et al. (2010; Fig. 5) were described and sampled for particle size, calcium carbonate ($CaCO_3$) and micromorphological analyses. These sections, corresponding to the Brown Laminated Clay (VC12-2), the Dark brown Waxy Laminated Clay (VC12-10) and the Light brown Sandy Laminated Clay (VC12-12) (VC12 = Victoria Cave and sampling year 2012, and marine isotope stage assigned by Lundberg et al., 2010), were described at the macroscale, and depths of samples are quoted as height above a flowstone (0 cm) at the base of each sequence. Given that large quantities of sediment were removed from the cave during the excavations of the 1870s, our samples were taken from the remaining thicknesses, which are unlikely to represent the original thicknesses present when the cave was discovered.

Samples for thin sectioning (micromorphology) were extracted in Kubiena tins (7.5 × 6 cm). Thin sections were prepared using the standard preparation techniques detailed by Palmer et al. (2008a) and described using the notation for lamination types and lamination sets proposed by Palmer et al. (2019). Bulk samples for particle size and $CaCO_3$ determinations were taken at 5 cm intervals for VC12-2 and VC12-10, and 10 cm intervals for VC12-12. Particle size analysis was performed using a Malvern Mastersizer 2000 with a Hydro MU sampling system. Single samples were measured five times, and the average grain size for each phi interval was used as the result. $CaCO_3$ was measured using a Bascomb Calcimeter, following the method of Avery and Bascomb (1982).

Sediment mineralogy was determined on legacy samples from each of the four laminated units identified in the stratigraphy of Lundberg et al. (2010; Figs. 2 and 5). No separation of the coarse and fine laminae was undertaken, as Murphy and Lord (2003) demonstrated that particle size variation is a textural rather than mineralogical characteristic. Analyses were conducted using a Bruker D8 X-ray diffractometer (XRD) along with Bruker Eva software. Sample preparation consisted of grinding to <75 μm.

Two samples, from the upper and lower parts of the Brown Laminated Clay (VC12-2) (Fig. 6), were collected for optically stimulated luminescence (OSL) dating by inserting plastic tubes horizontally into the sediment. The 4–11 μm silt fraction of each sample was isolated using Stokesian settling times. This fraction was then treated (over 28 days) with 30% H_2O_2 to remove organics, 37.5% HCl to remove carbonates and 35%

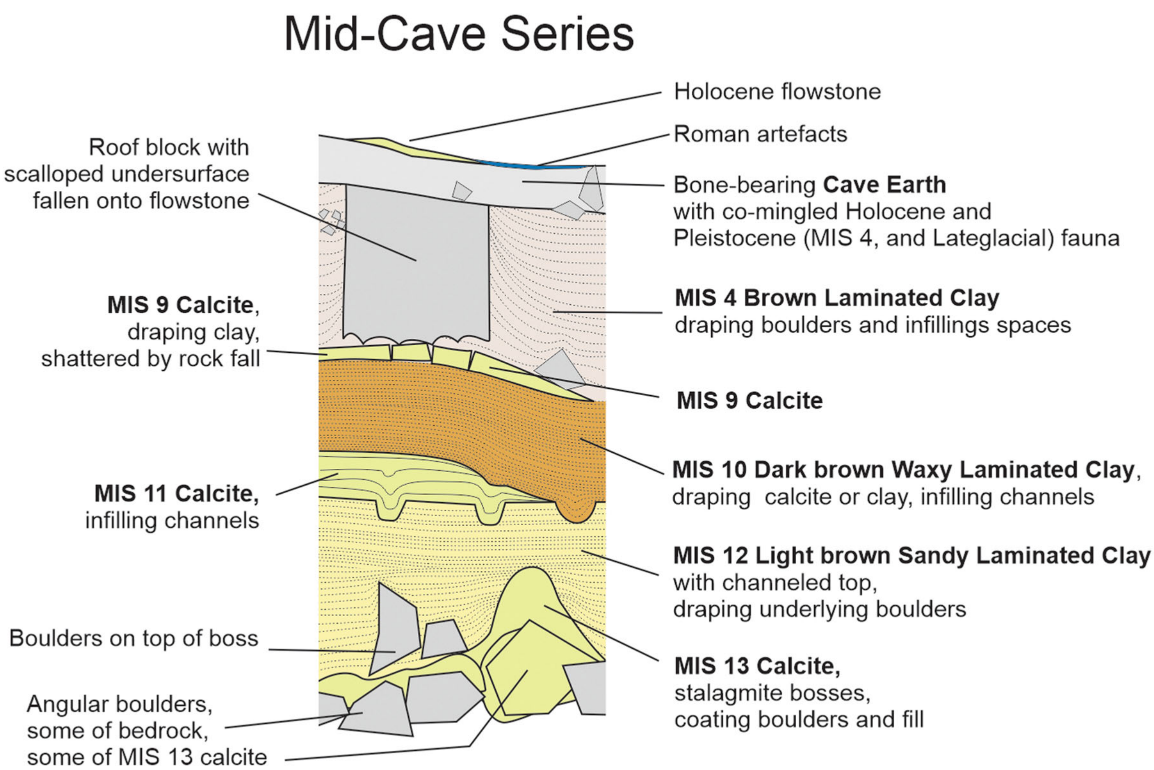

Figure 5. The Victoria Cave sedimentary sequence for the mid-cave area of excavation in 1870–1878 and 1937 (after Lundberg et al., 2010 and O'Connor and Lord, 2013). The samples for the current study were taken from the Light brown Sandy Laminated Clay, the Dark brown Waxy Laminated Clay and the Brown Laminated Clay. Note that the Bone-bearing Cave Earth, from which the ^{14}C ages were obtained, and Brown Laminated Clay, from which the OSL age was obtained, have been re-interpreted in light of the results of the present study, as outlined in Results and Discussion. [Color figure can be viewed at wileyonlinelibrary.com]

H_2SiF_6 to remove feldspars. The remaining silts were evaporated onto aluminium discs from suspension prior to measurement. Dosimetry was provided by Inductively Coupled Plasma Mass Spectrometry/Atomic Emission Spectrometry (ICP-MS/-AES) (Fig. 7), with uncertainties estimated conservatively at 5% for potassium and 10% for uranium and thorium. Water content is assumed at 15% ± 5%, yielding an effective range of 5%–25% (at 2σ). Cosmic contributions to dose are considered negligible in view of the geomorphological setting that comprises an effective overburden of many metres of limestone.

The OSL age determinations were conducted at the Oxford Luminescence Dating (OLD) laboratory at the University of Oxford. Analysis was conducted on Risø TL-DA-15 automated readers, using modified Single Aliquot Regenerative (SAR) protocols (Murray and Wintle, 2000, 2003), at a test dose of 12.84 Gy. These incorporated standard quality checks, including recycling, recuperation and post-IR feldspar purity checks. The signal was integrated from the first 2.5 s of stimulation, with background taken from the last 10 s. Initial results, however, revealed very weak luminescence signals, with exceptionally dim natural OSL response to stimulation and negligible coherent growth, despite regenerative doses >200 Gy. Only one of the samples (that from the upper part of VC12-2) showed any sign of regenerative growth, but this was very noisy. This sample was re-analysed with an elevated test dose (33.94 Gy), as this was suspected to be the source of the majority of the scatter in the growth; from these re-analyses, 26 of 30 aliquots yielded acceptable, albeit still dim (the initial natural integral was typically only ~1.5× the background) (Fig. 7(A)), and somewhat scattered growth (Fig. 7(B)). However, the majority of aliquots showed no evidence of IRSL response, and growth continuing in excess of 250 Gy. Fits were achieved with a mixture of linear, saturating exponential-plus-linear and double saturating exponential, depending on the quality of fit. Whilst a true linear fit at the higher doses is not likely, in some instances, large uncertainties on the regeneration points indicated that this was the

Figure 6. Exposure of the Brown Laminated Clay (VC12-2) between fallen roof blocks, undergoing measurement of dosimetry by Inductively Coupled Plasma Mass Spectrometry/Atomic Emission Spectrometry (ICP-MS/-AES). [Color figure can be viewed at wileyonlinelibrary.com]

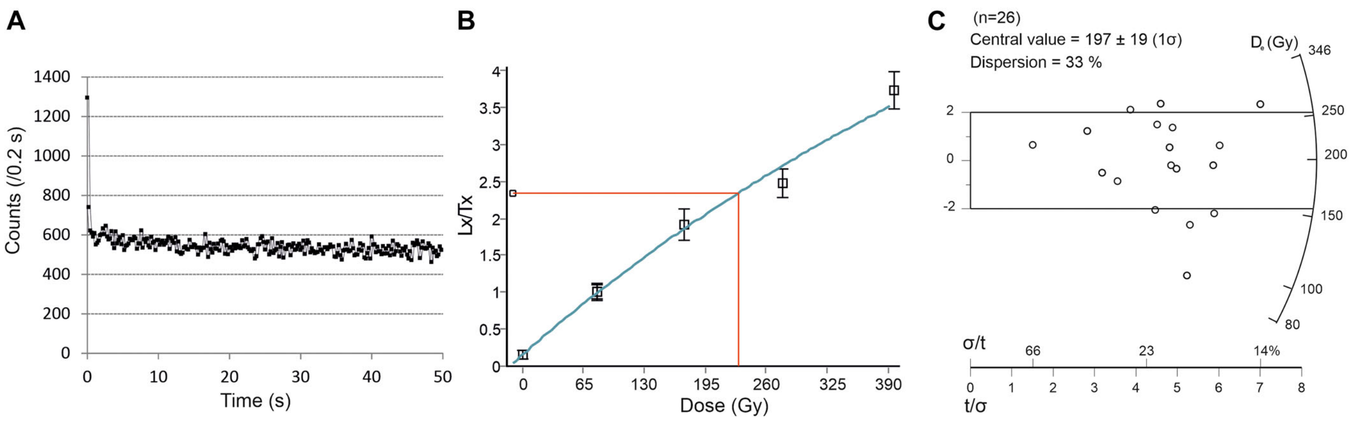

Figure 7. (A) Dim natural signal from the blue-stimulated (quartz) OSL response typical of the aliquots analysed. (B) Relatively large uncertainties and slightly inconsistent growth of the sample. (C) D_e estimates for the sample. [Color figure can be viewed at wileyonlinelibrary.com]

strongest fit, and on these grounds, it was retained. Whilst the overdispersion (33%) is far in excess of what would typically be expected for fine-grain silt analyses, it is considered more likely here to reflect the very poor typical signal/noise ratio of the OSL measurements, and resultant difficulties in accurately fitting the growth. Conversely, samples from areas with glacial histories are often characterised by dim luminescence response, with King et al. (2013) observing ~0.25% of grains providing a measurable signal. Where residual doses were observed in such settings, they were typically of the order of <10 Gy (King et al., 2013). Whilst it is often not possible to entirely rule out partial bleaching as a contributing factor to overdispersion, the equivalent dose (D_e) estimates show no pronounced skew (skewness = −0.03) (cf. Bailey and Arnold, 2006), and there is a lack of consistent form of $D_e(t)$ plots with increased signal integration time (Bailey et al., 2003). The dose distribution is shown in Fig. 7(C), and a single D_e estimate was thus calculated using the Central Age Model of Galbraith et al. (1999).

To amplify previous AMS ^{14}C dates for horse and reindeer from the Bone-bearing Cave Earth that overlies the Brown Laminated Clay (VC12-2, originally ascribed to MIS 2) (Lord et al., 2007; O'Connor and Lord 2013), a juvenile horse femur and a reindeer radius were submitted for AMS ^{14}C-dating. Between 0.5 and 0.6 g of bone powder was collected from each sample using a dental drill with a tungsten burr attachment. Collagen extraction was carried out at University College London (UCL) following the standard procedures of the Oxford Radiocarbon Accelerator Unit (ORAU) (AF method, Brock et al., 2010), which is based on a modified version of the Longin (1971) method. The ^{14}C dates were measured at ORAU. To denote the bone pretreatment at UCL rather than at ORAU, all measured dates were assigned 'OxA-V-wwww-pp' numbers, where 'wwww' indicates the wheel number and 'pp' is the position of the sample on the wheel (Brock et al., 2010). Background corrections were applied to our dates to account for the collagen extraction performed at UCL, following the method outlined by Wood, Bronk Ramsey, et al. (2010). A full description of our correction methodology can be found in Reade et al. (2020). Corrected dates are denoted by adding a 'C' to the end of the date code assigned by ORAU. Date calibration was performed using OxCal 4.4 (Bronk Ramsey 2020) and the IntCal20 data set (Reimer et al., 2020).

For pollen analysis, samples of ~40 g were taken from the same locations used for micromorphology (~2 cm from the upper and lower parts of each Kubiena tin). Twelve subsamples, of ~7.5 g each, were processed using standard procedures to remove carbonates, silicates and particles >150 µm (Moore et al., 1991). *Lycopodium* tablets were added to each sample to ascertain pollen concentrations, and the samples were scanned for the presence of palynomorphs.

Results

Macro-sedimentology

Brown laminated clay (VC12-2)

Unit 1a, which lies between 0 and 20 cm directly above the underlying flowstone (MIS 9), has very fine laminations alternating between silt and clay of approximately equal thickness. The laminations dip steeply (>60°) towards the back wall of the cave. There is normally a sharp contact between the silt and clay units, and between the clay and the silt. A graded transition from these very fine laminations to Unit 2, a massive silt, occurs at 20–27 cm and this grades into 2 cm of massive clay (Unit 3) at the top of the unit (Fig. 8). The $CaCO_3$ content ranges between 4% and 10%, with the highest values found in the upper part and at the base of the sequence. The grain size of the sediments is dominated by silt and clay throughout (Fig. 8), with the median grain size ranging between 4 µm and 12.35 µm. The highest percentage of clay is in the bulk samples 0–10 cm, corresponding with the clay-dominated facies at the base of the sequence. There is a small amount of very fine sand within two of the bulk samples, but this is less than 3% of the total sample.

Dark brown waxy laminated clay (VC12-10)

Unit 1a is in the lower 28 cm of this sequence, where the laminations are horizontally bedded and consist of alternations of very fine silt and clay, with the silt laminae being thinner than the clay layer, with sharp contacts between the laminae. Unit 1a grades into Unit 1, which is again composed of thin laminations, but with a higher silt content (Fig. 8). Unit 2 overlies this at 40–53 cm, and is a massive silt with some clay within it. The $CaCO_3$ content ranges between 0.2% and 12%, with the highest value in the middle of the sequence, ~20 cm above the base. The grain size of the bulk samples is dominated by very fine silt and clay (median = 3–7 µm) and, in comparison to VC12-2, there is a greater percentage of clay (10%–90%) in VC12-10 (Fig. 8). This increase in clay content is associated with a decrease in the silt component; where present, the sand content never exceeds 4%.

Light brown sandy laminated clay (VC12-12)

Unit 1a is characterised by a clay-dominated laminated deposit between 0 and 50 cm, with sharp contacts between the silt and the clay laminae, and between the clay and silt. There is a graded transition to Unit 1b, which lies between 50 cm and 120 cm, and is a more silt-dominated laminated facies (Fig. 8). Within the silt laminations gradation of the silt is visible and the clay laminations are of very fine thickness. Unit 1b is succeeded by 12 cm of massive silt with some clay within it (Unit 2), and transitions to Unit 3 through a graded contact with a darker unit above that is composed almost entirely of clay. The $CaCO_3$ content ranges between 0.7% and 11%; values exceeding 6% only occur between 40–75 cm and 100–140 cm. The median grain size ranges between 0.16 µm and 7.13 µm, and is thus dominated by very fine silt and clay. Sand is present throughout the sequence but is always less than 4% and only greater than 2% in bulk samples 30–35 cm and 140 cm (Fig. 8).

Micromorphology

Two lamination types additional to those proposed by Palmer et al. (2019) were identified from the thin sections. We have designated them LT xix, a clay that demonstrates multiple laminations of very fine silt normally grading to clay within the lamination, and LU via, a normally graded lamination from medium silt to fine silt that is well sorted and has a sharp upper contact. Three microfacies of the laminated sediments are evident (Fig. 8). Microfacies 1 is dominated by finer sediment grades and is generally found in association with Unit 1a. These are composed of very fine laminations, <2 mm thickness, with either a graded structure or a sharp contact between the silt and clay layers. There is always a sharp contact between the clay and the succeeding silt layer, with no disturbance along this contact. More complex structures occur within the coarser component of the lamination sets, where

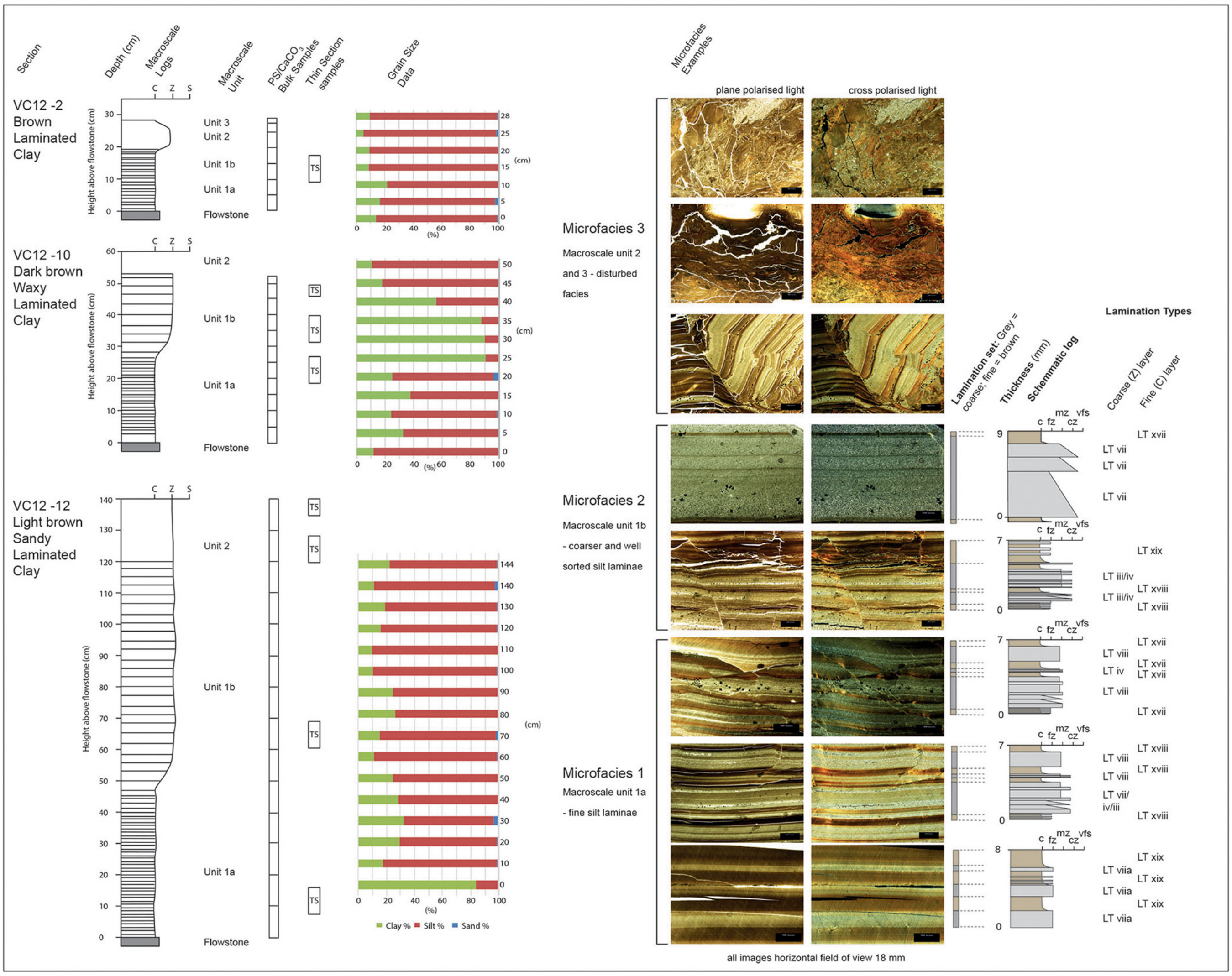

Figure 8. Macroscale description of the laminated sediment sequences from Victoria Cave showing the position of the bulk samples for grain size and $CaCO_3$ analyses, thin-section samples and particle size characteristics of bulk samples from each of the sections sampled. The sequences are dominated by silt-sized material, but with variations in the relative proportions of clay. The microfacies detected within the sequence are linked to the Units 1a, 1b and 2 in the macroscale description. Example schematic logs of the lamination types and sets of the microfacies are presented on the right-hand side, using the terminology of Palmer et al. (2019). [Color figure can be viewed at wileyonlinelibrary.com]

there are massive or graded silt laminae, 0.1–1 mm thick, of medium or coarse silt to fine silt with occasional laminae of massive, very coarse silt within these (LT iii/iv/via/vii/viii). The clay laminations, between 0.2 and 0.5 mm thick, tend to be massive with a masepic plasmic fabric under cross-polarised light (LT xviii/xix). There are similarities in the structures associated with the clay-dominated facies of VC12-2 and VC12-12, whereas this microfacies in VC12-10 tends to have fine silt in the coarser component of the lamination couplets, with no evidence of any coarser grain sizes within the silt layers. There is no evidence of current (flow) structures within the silt laminations; however, there is considerable evidence of normal faults within this microfacies.

The second microfacies is silt-dominated (Unit 1b; Fig. 8), where the coarser silt component is of a greater thickness (1–4 mm) than the associated clay lamination (0.1–0.5 mm). Again, the silt laminations comprise either massive coarse or medium silt, or graded structures from coarse silt to medium silt (LT iii/iv/vii). The contact between the silt and clay laminations is sharp or graded, whilst the clay to silt contact is sharp. The clay layers are normally massive and display a masepic plasmic fabric (LT xvi/xviii/xix). Again, these sediments are often normally faulted, with a unistrial fabric developed along the planes of displacement, but also towards the top of the microfacies, they are dominated by brecciated lenses of laminated sediment with the same characteristics as this second microfacies.

The third microfacies (Unit 2; Fig. 8) is composed of a partially homogenised silty clay with inclusions of small clay fragments (<2–4 mm a-axis), which retain some laminated structure within them, chaotically distributed within a predominantly very fine sand or silt matrix. In parts, the sediment has become completely homogenised and is a massive silty clay, although with strong masepic and unistrial plasmic fabrics within the unit.

Mineralogy

The four units of laminated sediment have remarkably consistent mineralogy. All samples consist principally of quartz and calcite, with minor amounts of chlorite, kaolinite and muscovite. Results from the three units from the Mid-Cave Series are shown in Fig. 9.

OSL dating

With the caveats around the weakness of the OSL signal in the sample reflecting large uncertainty on the

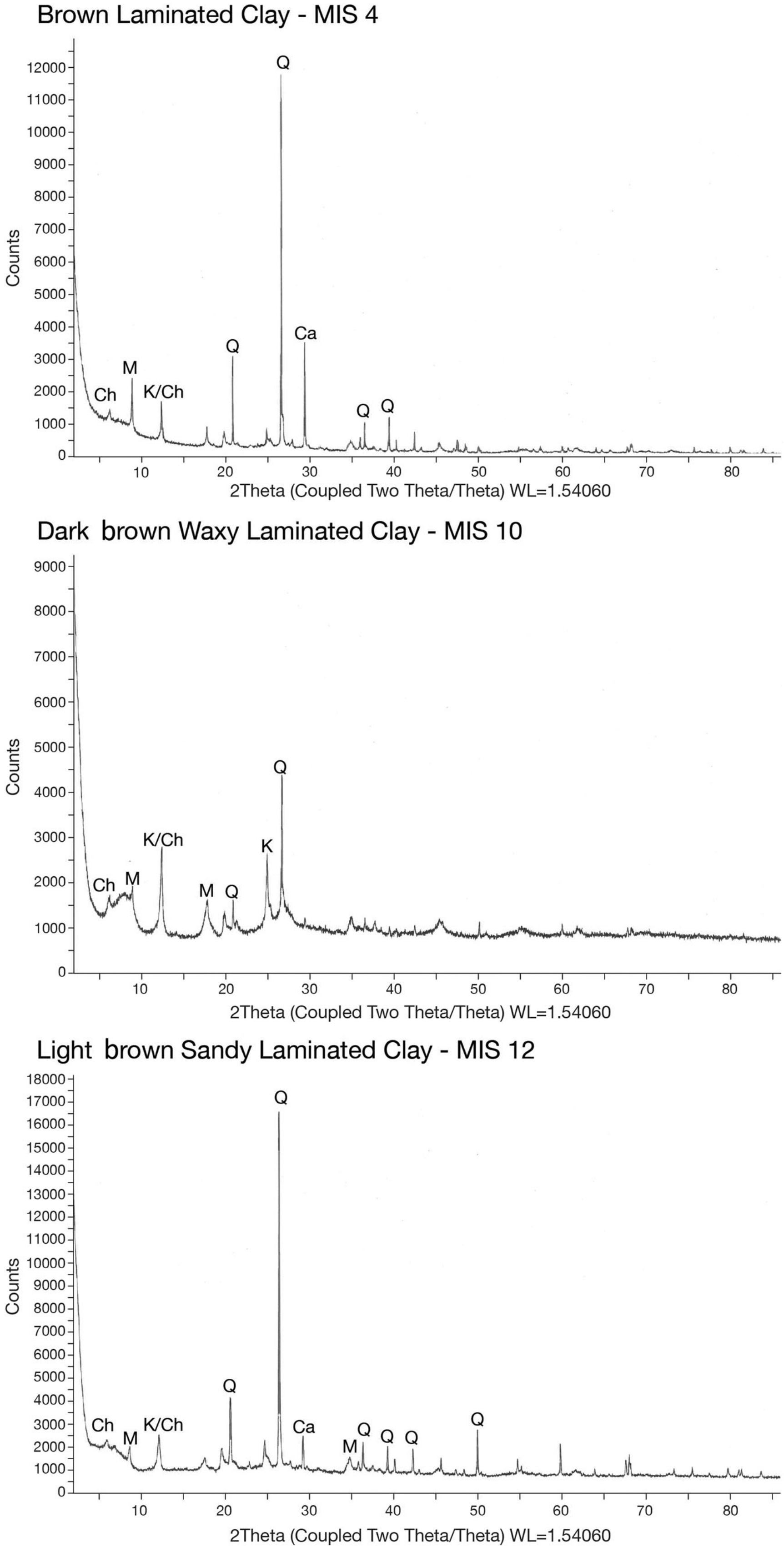

Figure 9. X-ray diffraction results for the three units of laminated sediments from the Mid-Cave Series. Letter codes: Ca, Calcite; Ch, Chlorite; K, Kaolinite; M, Muscovite; Q Quartz. The unit labelled MIS 4 was previously assigned to MIS 2 by Lundberg et al. (2010).

final age (relative standard deviation of 13%), an age of 66 ± 8.4 ka (1σ uncertainty) is considered most likely for the upper part of the Brown Laminated Clay (VC12-2). This age falls within MIS 4. Relevant data are summarised in Table 1.

AMS ^{14}C dating

Details of the AMS ^{14}C ages are summarised in Table 2. The juvenile horse returned an age of 46.1–54.9 cal. ka BP (OxA-V-2754-16C) and the reindeer returned an age of

48.9–>55.0 cal. ka BP (OxA-V-2798-15C). These ages are the 2σ uncertainty range and fall within the early part of MIS 3.

Pollen

Scans performed during the preparation process failed to reveal the presence of any pollen or spores. Observation of the prepared slides revealed only a mineral component together with the added *Lycopodium* spores.

Discussion

Mechanism of sediment emplacement

Laminated sediments have been reported from caves across the globe in landscapes affected by Quaternary cold-climate conditions, where they are explained by pulsed deposition in ice-dammed water bodies, for example, Norway (Valen et al., 1995, 1996), New Zealand (Williams, 1996), Austria (Audra et al., 2002), North America (Ward et al., 2003; Wood, Foreman et al., 2010; Munroe et al., 2016) and Spain (Ballesteros et al., 2017; Bartolomé et al., 2021). They have also been reported from caves in a number of karst landscapes in Britain and Ireland (Bull, 1981; Gale et al., 1985; O'Driscoil and Jennings, 2004; Waltham and Murphy, 2013). Laminated sediments in cave systems at the margin of the British MIS 2 ice sheet in South Wales (Bull, 1981) are now attributed to hydrological rejuvenation and pulsed deposition of fines during the much earlier and more extensive MIS 12 glaciation (Farrant et al., 2014). Victoria Cave is exceptional in preserving laminated sediments from multiple glacial–interglacial cycles (Lundberg et al., 2010).

In several cases, it has been proposed that during glacial episodes, cave entrances became blocked and partly or wholly invaded by ice. Meltwater lakes then formed inside some of these caves and acted as sediment traps, enabling fine-grained materials to settle from suspension and accumulate as distinct beds of silt and/or clay. Laminated units are regarded as varves if a seasonal sedimentation regime of alternating coarse (summer) and fine (winter) layers prevailed. This may have been the situation at Victoria Cave, but because we cannot demonstrate conclusively that the laminations relate to such a seasonal pattern, we therefore prefer to term them rhythmites.

We consider that the rhythmites accumulated by fall-out from suspension in water bodies that formed in the cave because of repeated damming by glacial ice that extended across the entrance to the cave during Late Pleistocene cold stages (cf. Valen et al., 1995, 1996; Williams, 1996; Ward et al., 2003; Wood, Forman et al., 2010; Munroe et al., 2016). The persistent deposition of finer sediment grades clearly indicates a low-energy, quiescent sedimentary environment with low-velocity flows forming currents in the lake. There is evidence of pulses of sediment entering the lake during extremely quiescent conditions of no current flow, enabling the deposition of clay, although there is some evidence of very low energy flows interrupting these periods of clay deposition (microfacies 1 and 2). The system is dominated by suspension settling from a plume of fine-grained sediments that are distributed within the water column. This is supported by the rhythmites draping over the underlying topography, including fallen roof blocks and former drainage channels, and with no persistent evidence of ripples or cross-bedding. Thus, they do not conform to sediment deposition from water flowing through a cave system, or a proximal sediment source such as ice releasing sediment into the lake.

We envisage a situation whereby during successive glacial stages, the southward-flowing Ribblesdale glacier passed across the mouth of the cave and possibly entered a short distance into it, and supplied and re-supplied to the interior sediment-laden meltwater from which the rhythmites were deposited. The persistent presence of clay within microfacies 1 and 2 with very sharp contacts between the clay and the succeeding silt layer, alternations between silt layers and clay layers, and multiple graded laminations in the silt layers are similar to the sediment structures reported in glaciolacustrine annually laminated sediments (Palmer et al., 2008b, 2019, 2026). However, invoking a similar interpretation here is difficult, since the annual cycle of sedimentation has not been demonstrated in analogue systems. Certainly, structures have developed with similar properties, but in microfacies 1, there are multiple examples of alternations between very fine silt and clay in the clay layer that would suggest that if they were deposited in the non-melt season, there were persistent low-energy flows during this period. Often, the transitions between the final coarse lamination before the clay layer are graded as well.

Nonetheless, these microfacies do demonstrate that these sediments were deposited initially in a very low energy sedimentary setting predominantly through suspension settling, although there is a slight but consistent increase in grain size either reflecting the infilling of the basin or the sediment source being more energetic or closer to the point of sedimentation. The lack of other sections within these basins makes this difficult to test.

The normal faults observed in the rhythmites are likely to result from compaction and/or settling of the sediments. In

Table 1. OSL details for the single sample that proved dateable from Victoria Cave.

Dosimetry	Grain size (μm)	4–11
	K content (%)	2.49 ± 0.13
	U content (ppm)	2.12 ± 0.21
	Th content (ppm)	2.12 ± 0.21
	Assumed water content (%)	15 ± 5
	Total dose rate (Gy ka^{-1})	2.99 ± 0.25
Equivalent dose estimation	Number of aliquots analysed/ accepted	26 (30)
	Central age model (Gy)	197 ± 19
	Overdispersion (%)	33
Age ± 1σ (ka)		66 ± 8.4

Table 2. AMS ^{14}C ages for horse and reindeer from Victoria Cave.

Museum/Excavation sample number	Species	Element	Laboratory code	Uncalibrated ^{14}C age ka	Calibrated 2σ age range ka
VC/762 1870–1878. Upper cave earth preservation type, UPN-353	Horse (*Equus ferus*)	Juvenile femur	OxA-V-2754-16C	46.4 ± 1.4	46.1–54.9
VC 100. Upper cave earth preservation type. Cave interior A/VC/B/2. UPN-361	Reindeer (*Rangifer tarandus*)	Radius	OxA-V-2798-15C	49.4 ± 2.1	48.9–>55.0

contrast, the brecciated lenses of laminated sediment in microfacies 2 and the homogenised silty clay with inclusions of chaotically distributed small clay fragments (<2–4 mm a-axis) in microfacies 3 may indicate either disruption by frost following ice withdrawal, drainage of the water body and exposure of the sediments or glaciotectonic deformation, as ice pressure at the cave entrance was released and caused disturbance of the sediments.

Sources of the laminated sediments

The presence of quartz and calcite in the rhythmites (Fig. 9) suggests that they consist of grains derived predominantly from the local Carboniferous limestones, sandstones of the Yoredale Series and/or the Millstone Grit. The presence of chlorite in all samples is most likely to derive from the Lower Palaeozoic rocks that crop out as an inlier in Ribblesdale, north of Victoria Cave. If this is correct, it indicates that these rocks were exposed prior to MIS12, when the Light brown Sandy Laminated Clay was deposited. Chlorite minerals are ubiquitous in low- and medium-temperature metamorphic rocks. They are diagnostic mineral species of the zeolite and lower greenschist metamorphic facies to which the Lower Palaeozoic strata of the Ribblesdale inlier belong. This supports previous geomorphological reconstructions of the area that indicate that the Lower Palaeozoic inlier up-ice from Victoria Cave was exposed by 440 ka BP, and most likely much earlier (Waltham, 2013).

Age determinations and significance

There are three lines of evidence that the rhythmite previously attributed to MIS 2 (the Brown Laminated Clay in Figs. 2 and 5) accumulated in MIS 4. The first is based on the OSL age of 66 ± 8.4 ka (Table 1). Although this single age should perhaps be treated with caution, given the caveats outlined above, other lines of evidence indicate that it is valid, suggesting that the rhythmite formed during a period of extensive glaciation in northern England during MIS 4.

Second, the OSL age is supported by the ^{14}C ages of 46.1–54.9 cal. ka BP for horse and 48.9–>55.0 cal. ka BP for reindeer (Table 2) from the overlying Bone-bearing Cave Earth (Tiddeman, 1876, 1877). Both ages are stratigraphically consistent with the OSL age and fall within the early part of MIS 3 (~59–28 ka). These two AMS-dated specimens are the first evidence of MIS 3 fauna from Victoria Cave. They demonstrate that the interior of Victoria Cave was open in early MIS 3 and the Bone-bearing Cave Earth overlying the MIS 4 rhythmite has a history of faunal inputs beginning much earlier than hitherto recognised. Previous studies considered the oldest fauna in this Bone-bearing Cave Earth to be of Lateglacial Interstadial age (14.7–12.9 cal. ka BP) (Lord et al., 2007; Lundberg et al., 2010; O'Connor and Lord, 2013). The early MIS 3 AMS-dated horse and reindeer from Victoria Cave also provide a new and rare record for components of the MIS 3 Pin Hole Cave Mammal Assemblage Zone (MAZ) in Currant and Jacobi's (2011) Late Pleistocene mammalian biostratigraphy. Victoria Cave is now the only site from the area subsequently covered by MIS 2 ice in northern England with AMS-dated MIS 3 mammalian fauna (Dinnis et al., 2016).

The recognition of early MIS 3 faunal inputs described here provides the third line of evidence supporting MIS 4 glaciation. Because MIS 2 glaciation removed older deposits at the cave entrance, we lack sediments showing events at the cave entrance before MIS 2. However, the presence of dated MIS sub-stage 5e bone deposits within the cave (Gascoyne et al., 1981; Gilmour et al., 2007; Lundberg et al., 2010; Fig. 3) demonstrates that the cave entrance was open in early MIS 5. The MIS 5 faunal record for Victoria Cave clearly shows inputs during sub-stage 5e, but very little, if anything, afterwards (Tiddeman, 1876). Recent work (Lundberg et al., 2020) at Stump Cross Caverns, 40 km east of Victoria Cave (Fig. 1(A)), indicates that reindeer and other boreal species were present in the region by ~90 ka BP. These species are characteristic of the late MIS 5 Banwell Bone Cave Mammal Assemblage Zone (MAZ) (Currant and Jacobi, 2011; Stevens and Reade, 2021). However, this fauna appears to be missing from Victoria Cave, Tiddeman (1876, 1877) reporting that reindeer is only found above the rhythmite now OSL-dated to MIS 4. Possibly, scree accumulation had blocked the cave entrance before the arrival of the Banwell Bone Cave MAZ, in which case, substantial scree would have been present by the end of MIS 5 ~ 71 ka.

Substantial clastic deposits attributable to MIS 5 are described by Tiddeman (1873) in the deep shaft dug just inside the cave entrance in 1872. It went down through ~2 m of rhythmites, now assigned to MIS 4, and then continued through unsorted clastic sediments for a further 6 m, before encountering the MIS 5e bone deposits. Tiddeman's (1873, 1875) sections appear to show the backslope remnants of truncated late MIS 5 scree cones that spilled into the cave from outside, augmented by roof collapse within the cave itself, prior to the formation of the MIS 4 rhythmite. We infer that the resumption of faunal inputs in early MIS 3 was made possible by MIS 4 glacial erosion removing scree deposits at the entrance and reopening the cave.

Dated flowstones from Stump Cross Caverns indicative of regional ice-free conditions constrain the uncertainty associated with the OSL age of 66 ± 8.4 ka for the Victoria Cave rhythmite (Fig. 10). Calcite flowstones are important environmental proxies (Fairchild and Baker, 2012). They form where drip waters charged with dissolved calcium carbonate enter ventilated open cave spaces. Vegetation and soil CO_2 at the surface enhance limestone dissolution by percolating waters, so that ice-free surface conditions are a pre-requisite for their formation. The dated flowstone sequence at Stump Cross Caverns (Baker et al., 1996; Lundberg et al., 2020) shows Late MIS 5 calcite formation terminating at the MIS 5a–MIS 4 transition ~71 ka and resuming at the MIS 4–MIS 3 transition ~59 ka. These phases of flowstone growth provide evidence for ice-free surface conditions, suggesting that the growth and decay of a regional ice sheet took place during the MIS 4 cold stage.

Published evidence from around the world for MIS 4 glaciation has been examined and discussed by Hughes et al. (2013) and Doughty et al. (2021) and, more specifically for central and northern Europe, by Helmens (2014): these review a wealth of proxy data that strongly supports the concept. In addition, ice-rafted debris records and Greenland ice core data indicate a period of severe and sustained cold with extensive glacial ice present in the North Atlantic region at that time (Hibbert et al., 2010; Wolff et al., 2010; Rasmussen et al., 2014; Fabian et al., 2023; Toucanne et al., 2023) (Fig. 10).

Given the rhythmite MIS 4 OSL age, the early MIS 3 ^{14}C dates for horse and reindeer from above the rhythmite and the resumption of faunal inputs in early MIS 3, we argue in favour of an extensive glaciation in northern England during MIS 4. Although we are not the first to make this claim, we are the first to provide local terrestrial-based dating evidence in support of the proposal.

Mitchell (2013) briefly assessed the evidence for MIS 4 glaciation in northern England and concluded that the severely cold climate indicated by the speleothem record from caves in North Yorkshire (Baker et al., 1993) was likely to correlate with

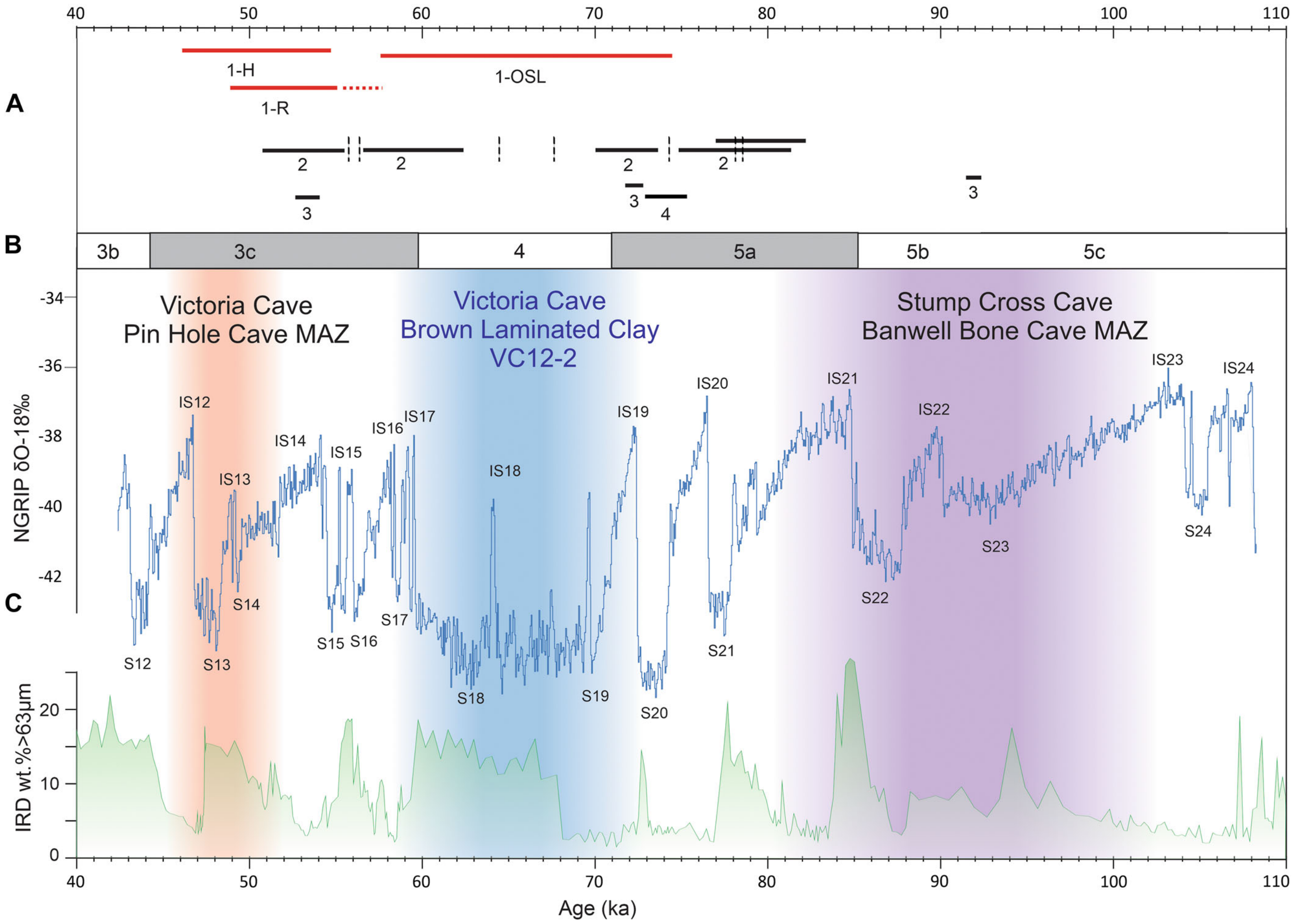

Figure 10. (A) Dates from Victoria Cave (red) and Stump Cross Caverns (black) shown as horizontal bars in relation to Marine Isotope Stages. (B) (Railsback et al., 2015) and NGRIP δO-18‰ (NGRIP project members 2004). (C) Greenland Stadials (S) and Interstadials (IS) (Rasmussen et al., 2014) and Ice Rafted Debris (IRD) from North Atlantic core KN166-14-JPC-13 (Hodell et al., 2010). Date identifiers are as follows: 1. This study: OSL date on laminated sediment (1-OSL), ^{14}C dates on horse (1-H) and reindeer bone (1-R); 2. Baker et al., 1996, Stump Cross Caverns, dated flowstones (horizontal bars) separated by non-dated sediment bands (vertical dashed lines); 3. Lundberg et al., 2020, Stump Cross Caverns flowstones; 4. Gilmour et al., 2007, Stump Cross Caverns, flowstone overlying Banwell Bone Cave MAZ. Dates are shown as two sigma range for calibrated ^{14}C, one sigma range for OSL and two sigma range for flowstones (where several dates are available on the same flowstone growth layer, the bar shows the period of continuous flowstone accumulation). [Color figure can be viewed at wileyonlinelibrary.com]

at least a locally extensive cover of glacial ice. Scourse (2024) reviewed the published data pertaining to the likelihood of MIS 4 glaciation in Britain and Ireland, and concluded that there is a convincing case in support of a major ice sheet over the uplands of western Britain and over Ireland at that time. In particular, surface exposure ages (^{26}Al and ^{10}Be) from mountain summits in North Wales indicate that these were overrun by ice during MIS 4 but not in MIS 2 (Hughes et al., 2021, 2022), implying thicker ice in the earlier period. There is also clear sediment stratigraphic and dating evidence for an Early Devensian glaciation in North Wales (Addison and Edge, 1992). Similarly, on Lundy Island at the entrance to the Bristol Channel in southern Britain, ^{26}Al and ^{10}Be ages indicate the probable existence of ice in MIS 4 (Rolfe et al., 2012). In the south of Ireland, OSL ages on raised beach sediments support the presence of an Irish ice sheet in MIS 4 (Gallagher et al., 2013). Likewise, Simms et al. (2025) reported OSL ages from a raised marine terrace in western Scotland that indicate the likely presence of a Scottish ice sheet during MIS 4.

The full extent across Britain of this proposed ice sheet is not yet known, but Batchelor et al. (2019) consider that it covered a smaller area than at the maximum of the MIS 2 glaciation (~27–21 ka; Last Glacial Maximum). This is corroborated by Rex et al. (2023), who reported that at Arclid in Cheshire, 136 km south of Victoria Cave, sands deposited between 77 ka and 47 ka show no glacigenic affinities. Thus, the ice passing Victoria Cave in MIS 4 apparently did not extend as far south as Arclid, and nor did any meltwater derived therefrom have an influence at the latter location. This is in contrast to ice coverage in MIS 2, which is considered to have terminated some 40 km and 120 km, respectively, to the southeast and south of Arclid (Clark et al., 2022; Rex et al., 2023).

Acceptance of the MIS 4 OSL age and MIS 3 ^{14}C ages has implications for the subsequent later Pleistocene history of Victoria Cave. In particular, why is there an absence of MIS 2 rhythmites in the cave, given that ice is known to have covered the area at that time? Tiddeman (1876) states that parts of the cave were filled with sediment before the excavations began, and contemporary photographs show this. The rhythmite that we have OSL-dated and now assign to MIS 4 had filled part of the cave to the roof at its front (Fig. 3), thus reducing the space available for a proglacial water body in MIS 2. A sequence of Pleistocene sediments at Stump Cross Caverns is devoid of rhythmites, indicating that conditions of their formation are site-specific (Lundberg et al., 2020).

A revised stratigraphic sequence for the Victoria Cave sediments is shown in Fig. 11. This incorporates the new age of MIS 4, based on OSL dating, for the Brown Laminated Clay and the MIS 3 AMS ^{14}C ages for the faunal remains. This figure updates the original version published in Lundberg et al. (2010).

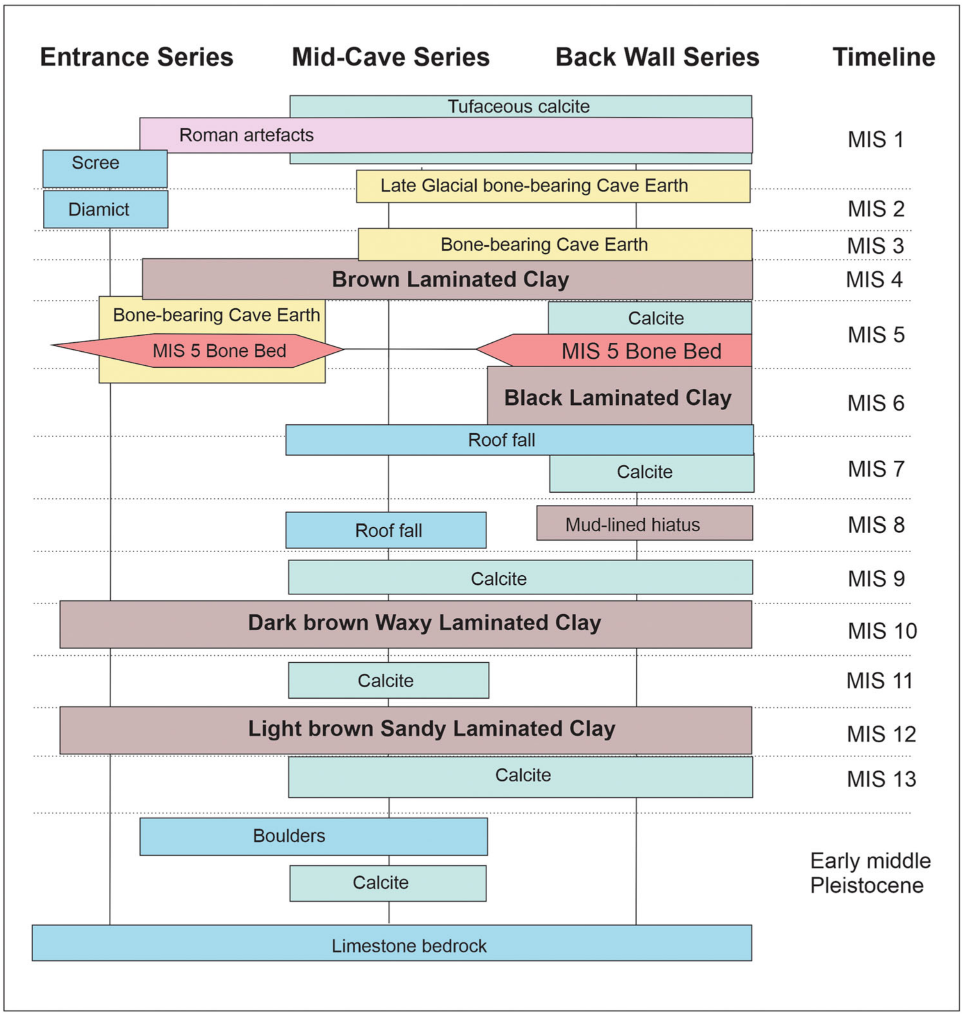

Figure 11. Revised stratigraphic summary for the sediments of the three main areas of Victoria Cave, incorporating the new age of MIS 4 for the Brown Laminated Clay, and the newly discovered MIS 3 faunal remains. This figure updates fig. 13 of Lundberg et al. (2010). [Color figure can be viewed at wileyonlinelibrary.com]

Conclusions

The OSL age of 66 ± 8.4 ka from the uppermost rhythmite unit in Victoria Cave constrains these sediments to MIS 4. This age is supported by AMS ^{14}C ages of 46.1–54.9 cal. ka BP and 48.9–>55.0 cal. ka BP for horse and reindeer, respectively, from the Bone-bearing Cave Earth that overlies the rhythmite unit (Fig. 10). These dates provide the first tightly constrained age for a cave rhythmite in Britain. The cave rhythmites are considered to have been deposited by fall-out from suspension in proglacial water bodies that formed as a consequence of repeated damming by glacial ice that extended across the entrance to the cave during Late Pleistocene cold stages. Arguably, these sediments are now the most intensively studied cave rhythmites in the world.

The MIS 4 age is significant in that it demonstrates glacial ice to have been more extensive than previously recognised in northern England at that time, and represents the first locally derived terrestrial-based dating evidence for that event. Furthermore, the stratigraphically consistent AMS ^{14}C ages for horse and reindeer indicate that the interior of the cave was open in early MIS 3, and faunal inputs above the MIS 4 rhythmite began much earlier than previously recognised. The absence of a MIS 2 rhythmite unit from the cave is attributed to a lack of accommodation space due to earlier emplaced sediments filling the cave to its roof. Thus, the rhythmites at Victoria Cave represent a record of all the glacial events after MIS 13 at ~480 ka, other than MIS 8 and MIS 2.

Acknowledgements. We thank Robert White, formerly of the Yorkshire Dales National Park Authority, for facilitating sampling at Victoria Cave, and the Yorkshire Dales Millennium Trust for funding the sampling. Professor Mark Bateman (University of Sheffield) provided valuable advice regarding the reliability of our OSL data. The comments of an anonymous referee and Professor Philip Hughes (University of Manchester) are appreciated.

Data availability statement

The data that support the findings of this study are available from the corresponding author upon reasonable request.

References

Addison, K. & Edge, M.J. (1992) Early Devensian interstadial and glacigenic sediments in Gwynedd, North Wales. *Geological Journal*, 27, 181–190.
Audra, P., Quinif, Y. & Rochette, P. (2002) The genesis of the Tennengebirge karst and caves (Salzburg, Austria). *Journal of Caves and Karst Studies*, 64, 153–164.
Avery, B.W. & Bascomb, C.L. (1982) *Soil Survey laboratory methods*, Technical Monograph 6. Harpenden: Soil Survey of England and Wales.
Bailey, R.M. & Arnold, L.J. (2006) Statistical modelling of single grain quartz D-e distributions and an assessment of procedures for estimating burial dose. *Quaternary Science Reviews*, 25, 2475–2502.
Bailey, R.M., Singarayer, J.S., Ward, S. & Stokes, S. (2003) Identification of partial resetting using De as a function of illumination time. *Radiation Measurements*, 37, 511–518.

Baker, A., Smart, P.L. & Edwards, R.L. (1996) Mass spectrometric dating of flowstones from Stump Cross Caverns and Lancaster Hole, Yorkshire: palaeoclimate implications. *Journal of Quaternary Science*, 11, 107–114.

Baker, A., Smart, P.L. & Ford, D.C. (1993) Northwest European palaeoclimate as indicated by growth frequency variations of secondary calcite deposits. *Palaeogeography, Palaeoclimatology, Palaeoecology*, 100, 291–301.

Ballesteros, D., Jiménez-Sánchez, M., Giralt, S., DeFelipe, I. & García-Sansegundo, J. (2017) Glacial origin for cave rhythmite during MIS5d-c in a glaciokarst landscape, Picos de Europa (Spain). *Geomorphology*, 286, 68–77.

Bartolomé, M., Sancho, C., Benito, G., Medialdea, A., Calle, M., Moreno, A. et al. (2021) Effects of glaciation on karst hydrology and sedimentology during the Last Glacial Cycle: the case of Granito cave, Central Pyrenees (Spain). *Catena*, 206, 105252.

Batchelor, C.L., Margold, M., Krapp, M., Murton, D.K., Dalton, A.S., Gibbard, P.L. et al. (2019) The configuration of Northern Hemisphere ice sheets through the Quaternary. *Nature Communications*, 10, 3713.

Brock, F., Higham, T., Ditchfield, P. & Ramsey, C.B. (2010) Current pretreatment methods for AMS radiocarbon dating at the Oxford Radiocarbon Accelerator Unit (ORAU). *Radiocarbon*, 52, 103–112.

Bronk Ramsey, C. (2020) *OxCal 4.4*. Oxford: Oxford Radiocarbon Accelerator Unit.

Bull, P.A. (1981) Some fine-grained sedimentation phenomena in caves. *Earth Surface Processes and Landforms*, 6, 11–22.

Chiverrell, R.C. & Thomas, G.S.P. (2010) Extent and timing of the Last Glacial Maximum (LGM) in Britain and Ireland: a review. *Journal of Quaternary Science*, 25, 535–549.

Clark, C.D., Ely, J.C., Hindmarsh, R.C.A., Bradley, S., Ignéczi, A., Fabel, D. et al. (2022) Growth and retreat of the last British-Irish Ice Sheet 31,000 to 15,000 years ago: the BRITICE-CHRONO reconstruction. *Boreas*, 51, 699–758.

Currant, A.P. & Jacobi, R.M. (2011) The mammalian faunas of the British Late Pleistocene. In: Ashton, N., Lewis, S.G. & Stringer, C. (Eds.) *The ancient human occupation of Britain*. Amsterdam: Elsevier, pp. 165–180.

Dearne, M.J. & Lord, T.C. (1998) *The Romano-British archaeology of Victoria Cave, Settle; researches into the site and its artifacts*. British Archaeological Reports. British Series, Oxford.

Dinnis, R., Pate, A. & Reynolds, N. (2016) Mid-to-late Marine Isotope Stage 3 mammal faunas of Britain: a new look. *Proceedings of the Geologists' Association*, 127, 435–444.

Doughty, A.M., Kaplan, M.R., Peltier, C., & Barker, S., (2021) A maximum in global glacier extent during MIS 4. *Quaternary Science Reviews*, 261, 106948.

Edwards, C.J., Ho, S.Y.W., Barnett, R., Coxon, P., Bradley, D.G., Lord, T.C. et al. (2014) Continuity of brown bear maternal lineages in northern England through the Last-glacial period. *Quaternary Science Reviews*, 96, 131–139.

Fabian, S.G., Gallagher, S.J. & de Vleeschouwer, D. (2023) British-Irish Ice Sheet and polar front history of the Goban Spur, offshore southwest Ireland over the last 250,000 years. *Boreas*, 52, 476–497.

Fairchild, I.J. & Baker, A. (2012) *Speleothem Science: From Process to Past Environments*. Chichester/Oxford: Wiley-Blackwell, p. 455.

Farrant, A.R., Smith, C.J.M., Noble, S.R., Simms, M.J. & Richards, D.A. (2014) Speleogenetic evidence from Ogof Draenen for a pre-Devensian glaciation in the Brecon Beacons, South Wales, UK. *Journal of Quaternary Science*, 29, 815–826.

Galbraith, R.F., Roberts, R.G., Laslett, G.M., Yoshida, H. & Olley, J.M. (1999) Optical dating of single and multiple grains of quartz from Jinmium rock shelter, northern Australia: part i, experimental design and statistical models. *Archaeometry*, 41, 339–364.

Gale, S.J., Hunt, C.O. & Southgate, G.A. (1985) The stratigraphy of Kirkhead Cave, an Upper Palaeolithic site in northern England. *Proceedings of the Prehistoric Society*, 51, 283–304.

Gallagher, C., Telfer, M.W. & Ó Cofaigh, C. (2015) A Marine Isotope Stage 4 age for Pleistocene raised beach deposits near Fethard, southern Ireland. *Journal of Quaternary Science*, 30, 754–763.

Gascoyne, M., Currant, A.P. & Lord, T.C. (1981) Ipswichian fauna of Victoria Cave and the marine palaeoclimatic record. *Nature*, 294, 652–654.

Gilmour, M., Currant, A., Jacobi, R. & Stringer, C. (2007) Recent TIMS dating results from British Late Pleistocene vertebrate faunal localities: context and interpretation. *Journal of Quaternary Science*, 22, 793–800.

Hedges, R.E.M., Housley, R.A., Bronk, C.R. & Van Klinken, G.J. (1992) Radiocarbon dates from the Oxford AMS system: archaeometry datelist 14. *Archaeometry*, 34, 141–159.

Helmens, K.F. (2014) The Last Interglacial-Glacial cycle (MIS 5-2) re-examined based on long proxy records from central and northern Europe. *Quaternary Science Reviews*, 86, 115–143.

Hibbert, F.D., Austin, W.E.N., Leng, M.J. & Gatliff, R.W. (2010) British Ice Sheet dynamics inferred from North Atlantic ice-rafted debris records spanning the last 175,000 years. *Journal of Quaternary Science*, 25, 461–482.

Hodell, D.A., Evans, H.F., Channell, J.E.T. & Curtis, J.H. (2010) Phase relationships of North Atlantic ice-rafted debris and surface-deep climate proxies during the last glacial period. *Quaternary Science Reviews*, 29, 3875–3886.

Hughes, P.D., Gibbard, P.L. & Ehlers, J. (2013) Timing of glaciation during the last glacial cycle: evaluating the concept of a global 'Last Glacial Maximum' (LGM). *Earth-Science Reviews*, 125, 171–198.

Hughes, P.D., Glasser, N.F. & Fink, D. (2022) ^{10}Be and ^{26}Al exposure history of the highest mountains in Wales: evidence from Y Wyddfa (Snowdon) and Y Glyderau for a nunatak landscape at the global Last Glacial Maximum. *Quaternary Science Reviews*, 286, 107523.

Hughes, P.D., Glasser, N.F., Fink, D., Dortch, J., Fülöp, R., Wilcken, K. et al. (2021) The timing of deglaciation from mountain summits to cirques in Wales: ^{10}Be and ^{26}Al exposure dates from Cadair Idris. In: *EGU General Assembly Conference Abstracts*, EGU21-10398.

Jacobi, R. & Higham, T. (2011) The later upper Palaeolithic recolonisation of Britain: new results from AMS radiocarbon dating. In: Ashton, N., Lewis, S.G. & Stringer, C. (Eds.) *The ancient human occupation of Britain*. Amsterdam: Elsevier, pp. 223–247.

Jacobi, R.M. & Lord, T.C. (2011) The earliest humans in the Yorkshire Dales National Park. In: Martlew, R.D. (Ed.) *Prehistory in the Yorkshire Dales, recent research and future prospects*. Yorkshire: Yorkshire Dales Landscape Trust, pp. 13–17.

King, G.E., Robinson, R.A.J. & Finch, A.A. (2013) Apparent OSL ages of modern deposits from Fåbergstølsdalen, Norway: implications for sampling glacial sediments. *Journal of Quaternary Science*, 28, 673–682.

Longin, R. (1971) New method of collagen extraction for radiocarbon dating. *Nature*, 230, 241–242.

Lord, T., Lundberg, J. & Murphy, P. (2012) A guide to work at Victoria Cave—from the 19th to 21st centuries. In: O'Regan, H.J., Faulkner, T. & Smith, I.R. (Eds.) *Cave archaeology and karst geomorphology of north west England: Field Guide*. London: Quaternary Research Association, pp. 84–97.

Lord, T.C., O'Connor, T.P., Siebrandt, D.C. & Jacobi, R.M. (2007) People and large carnivores as biostratinomic agents in Lateglacial cave assemblages. *Journal of Quaternary Science*, 22, 681–694.

Lundberg, J., Lord, T.C. & Murphy, P.J. (2010) Thermal ionization mass spectrometer U–Th dates on Pleistocene speleothems from Victoria Cave, North Yorkshire, UK: implications for paleoenvironment and stratigraphy over multiple glacial cycles. *Geosphere*, 6, 379–395.

Lundberg, J., Lord, T.C. & Murphy, P.J. (2020) New U-series dates from stump Cross Caverns, Yorkshire, UK, and constraints on the age of the Banwell Bone Cave Mammal Assemblage Zone. *Proceedings of the Geologists' Association*, 131, 639–651.

Mitchell, W.A. (2013) Glaciation and Quaternary evolution. In: Waltham, T. & Lowe, D. (Eds.) *Caves and karst of the Yorkshire Dales*, 1. Buxton: British Cave Research Association, pp. 29–64.

Moore, P.D., Webb, J.A. & Collinson, M.E. (1991) *Pollen analysis*, 2nd edition. London: Blackwell Scientific.

Munroe, J.S., Perzan, Z.M. & Amidon, W.H. (2016) Cave sediments constrain the latest Pleistocene advance of the Laurentide Ice Sheet in the Champlain Valley, Vermont, USA. *Journal of Quaternary Science*, 31, 893–904.

Murphy, P.J. & Lord, T. (2003) Victoria Cave, Yorkshire, UK: new thoughts on an old site. *Cave and Karst Science*, 30, 83–88.

Murray, A.S. & Wintle, A.G. (2000) Luminescence dating of quartz using an improved single-aliquot regenerative-dose protocol. *Radiation Measurements*, 32, 57–73.

Murray, A.S. & Wintle, A.G. (2003) The single aliquot regenerative dose protocol: potential for improvements in reliability. *Radiation Measurements*, 37, 377–381.

North Greenland Ice Core Project (NGRIP) members. (2004) High-resolution record of Northern Hemisphere climate extending into the last interglacial period. *Nature*, 431, 147–151.

O'Connor, T. & Lord, T. (2013) Cave palaeontology. In: Waltham, T. & Lowe, D. (Eds.) *Caves and karst of the Yorkshire Dales*, 1. Buxton: British Cave Research Association, pp. 225–238.

O'Drisceoil, C. & Jennings, R. (2004) Ballynamuck Caves 1 and 2. Available at: https://excavations.ie/report/2004/Waterford/0012783 [Accessed 9th May 2026].

Palmer, A.P., Bendle, J.M., Macleod, A., Rose, J. & Thorndycraft, V.R. (2019) The micromorphology of glaciolacustrine varve sediments and their use for reconstructing palaeoglaciological and palaeoenvironmental change. *Quaternary Science Reviews*, 226, 105964.

Palmer, A.P., Bendle, J.M., Matthews, I.P., Macleod, A., Staff, R.A. & Lincoln, P. et al. (2026) A varve chronology for glacial retreat and hydroclimate changes during Heinrich Stadial 1 on the northwest European margins. *Quaternary Science Reviews*, 376, 109771.

Palmer, A.P., Lee, J.A., Kemp, R.A. & Carr, S.J. (2008a) *Revised laboratory procedures for the preparation of thin sections from unconsolidated material*. Unpublished Internal Report. Royal Holloway, University of London.

Palmer, A.P., Lowe, J.J., Rose, J. & Walker, M.J.C. (2008b) Annually laminated Late Pleistocene sediments from Llangorse Lake, South Wales, UK: a chronology for the pattern of ice wastage. *Proceedings of the Geologists' Association*, 119, 245–258.

Quartermaine, J. (1995) *Victoria and Albert Caves, North Yorkshire, Archaeological Survey*. Lancaster, and Yorkshire Dales National Park: Lancaster University Archaeological Unit. p. 28.

Railsback, L.B., Gibbard, P.L., Head, M.J., Voarintsoa, N.R.G. & Toucanne, S. (2015) An optimized scheme of lettered marine isotope substages for the last 1.0 million years, and the climatostratigraphic nature of isotope stages and substages. *Quaternary Science Reviews*, 111, 94–106.

Rasmussen, S.O., Bigler, M., Blockley, S.P., Blunier, T., Buchardt, S.L., Clausen, H.B. et al. (2014) A stratigraphic framework for abrupt climatic changes during the Last Glacial period based on three synchronized Greenland ice-core records: refining and extending the INTIMATE event stratigraphy. *Quaternary Science Reviews*, 106, 14–28.

Reade, H., Tripp, J.A., Charlton, S., Grimm, S.B., Leesch, D., Müller, W. et al. (2020) Deglacial landscapes and the Late Upper Palaeolithic of Switzerland. *Quaternary Science Reviews*, 239, 106372.

Reimer, P.J., Austin, W.E.N., Bard, E., Bayliss, A., Blackwell, P.G., Bronk Ramsey, C. et al. (2020) The IntCal20 Northern Hemisphere radiocarbon age calibration curve (0–55 cal kBP). *Radiocarbon*, 62, 725–757.

Rex, C.L., Bateman, M.D., Buckland, P.C., Panagiotakopulu, E., Livingstone, S.J., Hardiman, M. et al. (2023) A revision of the British chronostratigraphy within the last glacial–interglacial cycle based on new evidence from Arclid, Cheshire UK. *Quaternary Science Reviews*, 299, 107882.

Rolfe, C.J., Hughes, P.D., Fenton, C.R., Schnabel, C., Xu, S. & Brown, A.G. (2012) Paired ^{26}Al and ^{10}Be exposure ages from Lundy: new evidence for the extent and timing of Devensian glaciation in the southern British Isles. *Quaternary Science Reviews*, 43, 61–73.

Scourse, J.D. (2024) The timing and magnitude of the British-Irish Ice Sheet between Marine Isotope Stages 5d and 2: implications for glacio-isostatic adjustment, high relative sea levels and 'giant erratic' emplacement. *Journal of Quaternary Science*, 39, 505–514.

Simms, A.R., Dewitt, R., Bradley, S.L., Huffman, E., Best, L., Bradwell, T. et al. (2025) Was Scotland covered by an ice sheet during Marine Isotope Stage 4? Insights from the pre-Last Glacial Maximum marine terraces of northwest Scotland. *Journal of Quaternary Science*, 40, 1097–1105.

Stevens, R.E. & Reade, H. (2021) Stable isotopes confirm the Banwell Bone Cave Mammal Assemblage Zone represents an MIS 5 fauna. *Quaternary Research*, 101, 245–255.

Tiddeman, R.H. (1872) On the evidence for the ice-sheet in north Lancashire and adjacent parts of Yorkshire and Westmoreland. *Quarterly Journal of the Geological Society of London*, 28, 471–491.

Tiddeman, R.H. (1873) The older deposits in the Victoria Cave, Settle, Yorkshire. *Geological Magazine*, 10, 11–16.

Tiddeman, R.H. (1875) The work and problems of the Victoria Cave exploration. *Proceedings of the Geological and Polytechnic Society of the West Riding of Yorkshire*, 10, 11–16.

Tiddeman, R.H. (1876) *Third report of the committee, consisting of Sir John Lubbock Bart., Prof. Prestwich, Prof. T. McK. Hughes, Prof. W. Boyd Dawkins, Rev. H.W. Crosskey, Messrs. L.C. Miall and R.H. Tiddeman, appointed for the purposes of assisting in the exploration of the Settle Caves (Victoria Cave), 1875*. Report of the Forty-fifth Meeting of the British Association for the Advancement of Science, Bristol. pp. 166–175.

Tiddeman, R.H. (1877) *Fourth report of the committee, consisting of Sir John Lubbock, Bart., Prof. Prestwich, Prof. Busk, Prof. T. McK. Hughes, Prof. W. Boyd Dawkins, Prof. Miall, Rev. H.W. Crosskey, and Mr R.H. Tiddeman, appointed for the purposes of assisting in the exploration of the Settle Caves (Victoria Cave)*. Report of the Forty-sixth Meeting of the British Association for the Advancement of Science, Glasgow, 1876. pp. 115–118.

Tiddeman, R.H. (1878) On the age of the hyaena-bed at the Victoria Cave, Settle, and its bearing on the antiquity of man. *The Journal of the Anthropological Institute of Great Britain and Ireland*, 7, 165–173.

Toucanne, S., Rodrigues, T., Menot, G., Soulet, G., Cheron, S., Billy, I. et al. (2023) Marine Isotope Stage 4 (71–57 ka) on the western European margin: insights to the drainage and dynamics of the western European Ice Sheet. *Global and Planetary Change*, 229, 104221.

Valen, V., Larsen, E. & Mangerud, J. (1995) High-resolution paleomagnetic correlation of Middle Weichselian ice-dammed lake sediments in two coastal caves, western Norway. *Boreas*, 24, 141–153.

Valen, V., Mangerud, J., Larsen, E. & Hufthammer, A.K. (1996) Sedimentology and stratigraphy in the cave Hamnsundhelleren, western Norway. *Journal of Quaternary Science*, 11, 185–201.

Waltham, T. (2013) Karst geomorphology. In: Waltham, T. & Lowe, D. (Eds.) *Caves and karst of the Yorkshire Dales*, 1. Buxton: British Cave Research Association, pp. 65–92.

Waltham, T. & Murphy, P. (2013) Cave geomorphology. In: Waltham, T. & Lowe, D. (Eds.) *Caves and karst of the Yorkshire Dales*, 1. Buxton: British Cave Research Association, pp. 117–146.

Ward, B.C., Wilson, M.C., Nagorsen, D.W., Nelson, D.E., Driver, J.C. & Wigen, R.J. (2003) Port Eliza cave: North American west coast interstadial environment and implications for human migrations. *Quaternary Science Reviews*, 22, 1383–1388.

Williams, P.W. (1996) A 230 ka record of glacial and interglacial events from Aurora Cave, Fiordland, New Zealand. *New Zealand Journal of Geology and Geophysics*, 39, 225–241.

Wolff, E.W., Chappellaz, J., Blunier, T., Rasmussen, S.O. & Svensson, A. (2010) Millennial-scale variability during the last glacial: the ice core record. *Quaternary Science Reviews*, 29, 2828–2838.

Wood, J.R., Forman, S.L., Everton, D., Pierson, J. & Gomez, J. (2010) Lacustrine sediments in Porter Cave, Central Indiana, USA and possible relation to Laurentide ice sheet marginal positions in the middle and late Wisconsinan. *Palaeogeography, Palaeoclimatology, Palaeoecology*, 298, 421–431.

Wood, R.E., Bronk Ramsey, C. & Higham, T.F.G. (2010) Refining background corrections for radiocarbon dating of bone collagen at ORAU. *Radiocarbon*, 52, 600–611.